TAO, Vol.4, No.1, 17-34, March 1993

A Preliminary Analysis of the Taiwan Hualien Radar Data

ALFRED T. C. CHANG[1], LONG S. CHIU[2],
TAI-CHI CHEN WANG[3], PAY-LIAM LIN[3] and GIN-RONG LIU[4]

(Manuscript received 25 August 1992, in final form 10 December 1992)

ABSTRACT

Two months of data collected by the meteorological radar in Hualien, Taiwan, and the available rain gauge data in the radar-covered area, are examined. These periods correspond to the times of the Algorithm Intercomparison Program conducted by the Global Precipitation Climatology Project in the Japan area. Statistical analysis showed little range dependence of radar reflectivity, in contrast to the findings of Petty and Katsaros for the Taiwan Area Mesoscale Experiment (TAMEX), indicating that the range dependence of the radar has been accounted for. A period of anomalously high reflectivity was detected. Infrared imagery from the GMS satellite showed the absence of cloud for the same period, suggesting the possibility of anomalous propagation (AP). Monthly mean radar rain rates compare favorably with the gauge averages, GOES Precipitation Index, and with Special Sensor Microwave Imager (SSM/I) estimates.

The threshold technique for estimating areal average rain rates proposed by Chiu and others was tested using Z-R relations typical of the Taiwan area. Despite the uncertainty in the Z-R relation and the VIP level processing of the radar, the variance of areal rain rate explained by the optimal threshold is about 90%.

Our analysis demonstrated the applicability of the threshold technique in estimating areal rainfall in the Hualien radar-covered area, and the use of IR observations in detecting AP. Higher spatial and temporal (at least every 15 minutes) resolution rain gauge observations and concomitant satellite visible, infrared, and/or microwave observations will prove to be vital to the advancement of quantitative rainfall estimation in Taiwan.

[1] Hydrological Sciences Branch, Goddard Space Flight Center, Greenbelt, MD 20771, U.S.A.

[2] General Sciences Corporation, Laurel, Maryland 20707, U.S.A.

[3] Atmospheric Sciences Department, National Central University, Chung-Li, Taiwan, R.O.C.

[4] Center for Space and Remote Sensing Research, National Central University, Chung-Li, Taiwan, R.O.C.

1. INTRODUCTION

The importance of tropical rainfall to global atmospheric circulation has been recognized, both theoretically and from observations. The Tropical Rainfall Measuring Mission (TRMM), initiated jointly by the U.S.A. and Japan, will pioneer the first international effort to measure tropical rainfall (Simpson *et al.*, 1988). A set of instruments, including a precipitation radar, a microwave radiometric sensing package, and infrared and visible scanners, has been assembled for the first time, in a coordinated effort, to probe the spectral characteristics and dynamic structures of tropical rainfall systems. From these measurements instantaneous rainfall rates can be derived. To validate these satellite estimates, parallel efforts to obtain surface measurements of rainfall by surface radar and/or rain gauges are on-going. These include radar sites in Darwin, Australia, the Kwajelein Atolls, Marshall Islands; Patrick Air Force Base, Florida, USA; and Puhket, Thailand.

In the tropics, precipitation brought about by meso-scale systems, such as typhoon or "Mei-Yu", affects men's activity from recreation planning, water resources management, and aviation operations to agricultural production. The need for accurate precipitation measurements has been realized in many countries. With a strong economy and a growing concern for the living environment, Taiwan has initiated a Space Research Program. One of the objectives of the program is the use of satellite data to improve weather forecasts and to monitor the environment.

To monitor typhoon and Mei-Yu activities, meteorological radars have been installed in Taiwan since 1970's. They included two S-band radars operated by the Central Weather Bureau (CWB), situated respectively in Kaohsiung and Hualien. These radar imageries have been used for the detection and prediction of typhoon paths and location of Mei-Yu fronts. They are, however, limited in their capability in quantitative rainfall estimates. Recently, these two radars have been upgraded and can now provide digitized reflectivity data. These digitized radar data open up opportunities for quantitative rainfall assessment, and promise potential contribution to the TRMM program.

A preliminary analysis of the digitized radar data in Kaohsiung has been made by Wang, *et al.* (1988). They compared the radar rain rates derived from the classical Marshall-Palmer Z-R relation to those measured by the rain gauges and found that the ratio of gauge rain rate to radar rain rate (G/R) is quite variable. They attributed the poor comparison to inadequate sampling by the rain gauges and radar.

A strong correlation between rain area above certain threshold and areal rainfall has been established, both empirically (Chiu 1988a,b, Rosenfeld *et al.*, 1990) and from theoretical considerations (Atlas *et al.*, 1989, Kedem *et al.*, 1990a). The ramification of this strong relation is that areal rainfall can be estimated by determining the rain area above certain threshold, if the climatology of the rain rate distribution is known. Chiu and Kedem (1990) pointed out that as long as there is a relationship between an observation such as microwave radiances or IR temperatures and rain rate, a linear relation exists between the areal average rain rate and areas above (or below) a certain threshold of the observable. This relationship is the basis of the Height Area Rainrate Threshold (HART) technique (Atlas, *et al.*, 1989), the Area Time Integral (ATI) technique (Doneaud *et al.*, 1984), and forms the underlining assumption of the GOES Precipitation Index (GPI) for rainfall estimation from IR data (Arkin, 1979, Arkin and Meisiner, 1987).

In this paper, an analysis of the Hualien radar data is presented. Two months of radar data from Hualien were analyzed. Monthly mean rain radar rates are compared with a rain index similar to the GPI and from rain rate estimated from the microwave measurements taken by the Special Sensor Microwave Imager (SSM/I) on board the Defense Meteorological Satellite Program (DMSP) satellites. The applicability of the threshold technique

in establishing areal average rainfall is examined using Z-R relations typical of the Taiwan summer. The sensitivity of the Z-R relations in establishing the relation between rain area and areal rainfall is tested. The inadequacy of rain gauge data in deriving a Z-R relation is demonstrated. Recommendations regarding effort to quantify rain rate estimates from the Hualien radar data are made.

2. DATA

Radar reflectivity and rain gauge data are used for our analysis. To compare the radar rain rates, rain rates estimated using infrared and microwave observations from other satellites are also included.

2.1 Hualien Radar Data

Characteristics of the Hualien radar are listed in Table 1. Reflectivity values are recorded in DVIP (Differential Video Integration and Processor) levels. The radar processing software remaps the volume scan reflectivity taken during the first 10 minutes of each hour (unless otherwise specified) to a Plan Position Indicator (PPI). The radar returns have been range corrected and external calibration of the radar return power is performed routinely. A column vector reflectivity in cartesian grid of size 4 km by 4 km (CV) is defined. the maximum reflectivity values (Z) within each vertical column of the cartesian grid are recorded. This is the reflectivity data available for our analysis.

Two time periods of radar data: (1) June 1-30, 1989 and (2) July 15-August 15, 1989, were selected. These time periods correspond to the time period of the Global Precipitation Climatology Program (GPCP) Algorithm Intercomparison Program (AIP) when data from the Japanese Geostationary Meteorological Satellite (GMS) were readily available to us. Due to the influences of the Central Mountain Range of Taiwan, only data observed between azimuths 30° and 190° relative to true north are used, as was done by Petty and Katsaros (1991). The effective areal coverage of the radar is depicted in Figure 1.

Table 1. Specification of the Taiwan Hualien radar.

Type	WSR-74S
Frequency	2.7-2.9 GHz
Wavelength	10.35-11.1 cm
Peak Transmitting Power	500 KW
PRF	539 pps and 164 pps
Pulse Width	0.5 usec and 4 usec
Antenna Diameter	12 feet
Beam Width	2.25 degree
PPI Display range	50, 125, 250, 500 km
RHI display range	50, 125, 250, 500 km

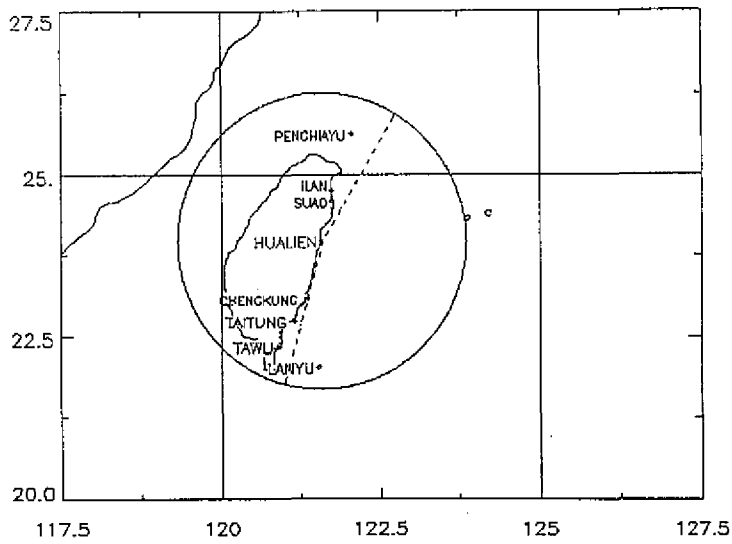

Fig. 1. Hualien radar coverage and location of rain gauge stations.

2.2 GMS Data

Infrared and visible imagery for the same period for Japan and the surrounding area have been assembled by the Global Precipitation Climatology Project (GPCP) for the Algorithm Intercomparison Program (AIP). Only the area north of 20°N of the radar-covered area is covered by the IR and visible imagery. The IR and visible data have been re-sampled onto 0.05° latitude by 0.0625° longitude grids. Hourly IR data are available. Visible data are only available hourly between 9 a.m. and 5 p.m., or 8 imageries per day.

2.3 Rain Gauge Data

Most of the operational rain gauges reside on Taiwan island. Hourly rain rate measurements at seven rain gauge stations, located respectively in Penchiayu, Suao, Ilan, Chengkung, Taitung, Tawu, and Lanyu, have been selected for our analysis. Figure 1 shows the locations of the rain gauges. Only hourly average gauge rain rates are recorded. Most of the rain gauge stations are outside the radar-covered area, with the exception of Lanyu, which is on the borderline.

3. DATA ANALYSIS

In this section, statistics of radar reflectivity are presented and the use of infrared imagery for the detection of anomalous propagation (AP) is discussed. The radar monthly mean rain rate computed using a simple reflectivity-rain rate (Z-R) relation are compared with other satellite and gauge rain rate estimates.

3.1 Range Dependence of Maximum Reflectivity

Maps of hourly maximum radar reflectivity for the first 10 minutes of each hour, Z, have been manually checked. Missing sectors and ground clutter have been deleted. Reflectivity measurements within 40 km of the radar station are considered ground clutter and excluded in our analysis. To examine the range degradation of the radar reflectivity, Figure 2 shows the arithmetic averaged Z as a function of range for these two time periods. The variation in dBZ as a function of distance is about 0.5 dBZ for the June period and 1 dBZ for the July/August period over the distance of 250 km. This finding differs from that of Petty and Katsaros (1991) who found a large range dependence of dBZ values (about 15 dBZ at a range of 200 km) for the Hualien radar data during TAMEX. This difference is probably due to the fact that the radar data they used for TAMEX are not range-corrected. Since the overall range difference in our analysis is less than 1 dBZ, no additional range correction was applied in this study.

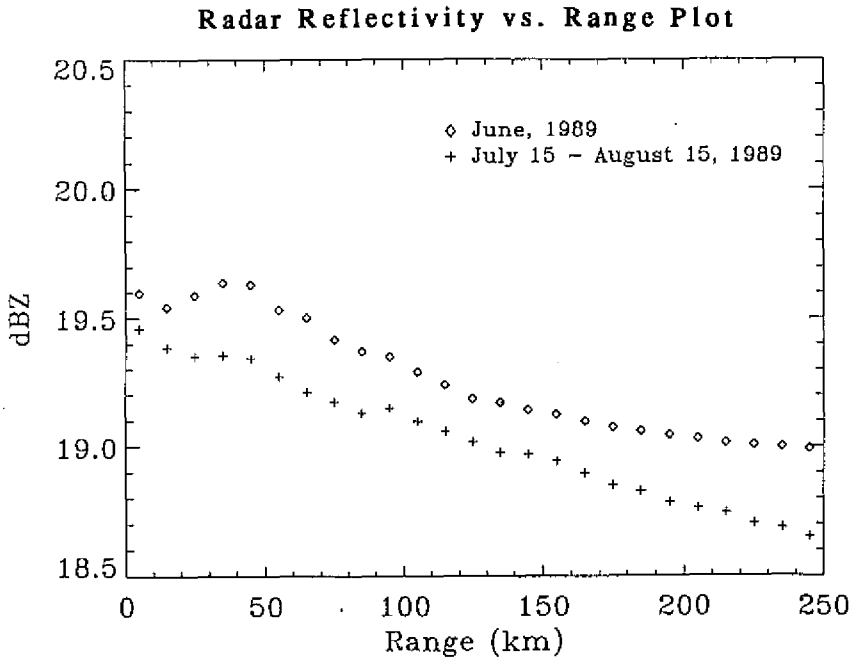

Fig. 2. Maximum radar reflectivity as a function of range for June 1-30, 1989 (a) and period 2, July 15-August 15,1989 (b).

3.2 Ground Clutter and Anomalous Propagation

Hourly radar maps show that from June 15 to 17, regions of high Z values in excess of 55 dBZ occur in the general area of the Iriomoto Jima. Figure 3a showed the map of columnar reflectivity for June 15. Another region of high columnar reflectivity values (in excess of 40 dBZ) appears in the south east quadrant. Examination of the corresponding GMS IR imagery for the same period (Figure 3b) showed the absence of clouds in the region.

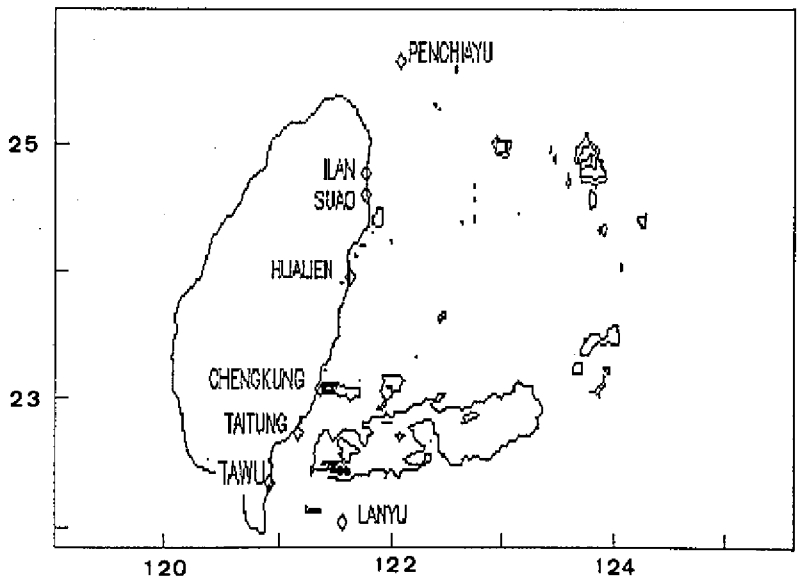

Fig. 3a. Radar reflectivity (Z) maps for June 15, 1989. The contour shows areas with dBZ values in excess of 55 dBZ. The anomalously high Z areas to the east and the south east quadrant are depicted.

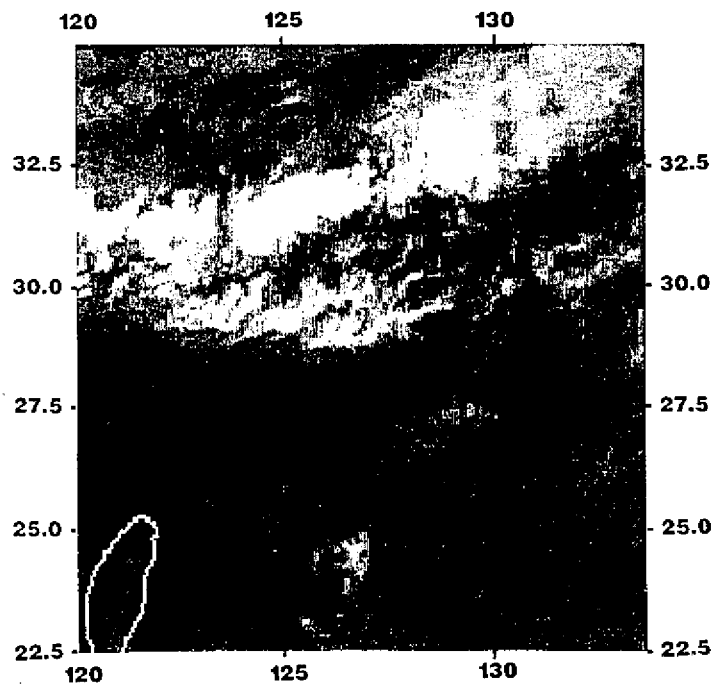

Fig. 3b. Infrared imagery from the GMS satellite for the same time as Fig. 3a. The absence of clouds in the areas of high radar reflectivity indicates the possibility of anomalous propagation.

During this period, the Taiwan area is dominated by southwesterly winds. Temperatures in most places are above normal, with little or no precipitation. The regions of high reflectivity depicted in the radar maps show the absence of clouds. Additionally, all seven rain gauges did not record any rain during this period (Figure 6a). Further examination of the radar data showed that the high Z values in the south east quadrant are stationary during the entire three day period. This is contrary to typical weather-related features and hence points to the potential of ground clutter or AP. These three days of data are removed from our analysis.

3.3 Probability Distribution of Maximum Reflectivity

Figure 4 shows the histograms of maximum reflectivity, in dBZ, for all pixels and scans for the June and July/August periods respectively. The fraction of pixels greater than 18 dBZ are 2.93% and 5.22% respectively for June and July/August period. It can be seen that the histograms are characterized by multiple peaks, which probably correspond to the VIP levels. The VIP data have found applications in flash flood warning and operational hydrology (Moore and Smith, 1979), but its applicability in detailed quantitative rainfall estimates may be limited.

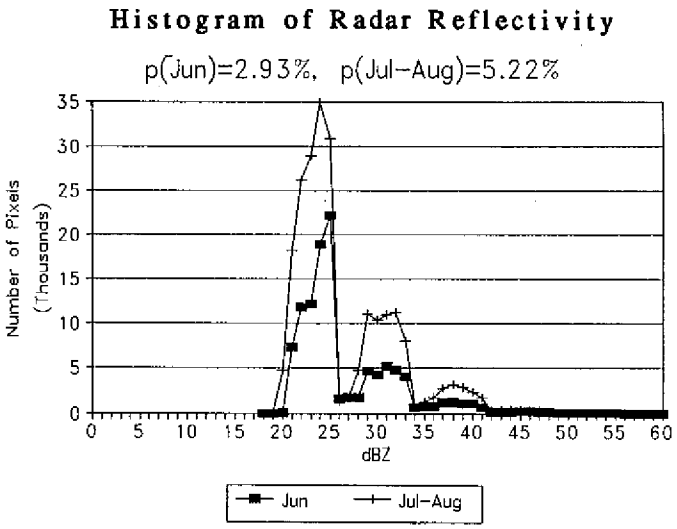

Fig. 4. Histograms of maximum reflectivity for June (square) and July-August (cross), 1989.

3.4 Rain Gauge Rain Rate Distribution

The location and total accumulation for each station for these periods are presented in Table 2. Examination of the hourly rain rates at the gauges shows large temporal variability. Total daily accumulations for all seven gauges have been computed. Figures 5a and 5b show the times series of the average daily accumulation for all seven gauges. Rain events occur in pulses, separated roughly 3-10 days apart. The monthly sum for all seven stations for the June (30 days) and July-August (32 days) periods are respectively, 66 and 293 mm, reflecting the dry condition in June and a return to normal during July and August.

Table 2. Location and Total Accumulation of Rain Gauge Stations.

Station	Lat.(N)Long.(E)	June Total (mm)	July-August Total
Suao	24°36' 121°45'	165.5	300.0
Ilan	24°46' 121°45'	67.4	308.0
Tawu	22°21' 120°54'	30.0	404.6
Taitung	22°45' 121°09'	5.1	487.3
Lanyu	22°02' 121°33'	123.0	259.5
Chengkung	23°06' 121°22'	26.0	326.4
Penchiayu	25°38' 122°04'	47.1	100.1

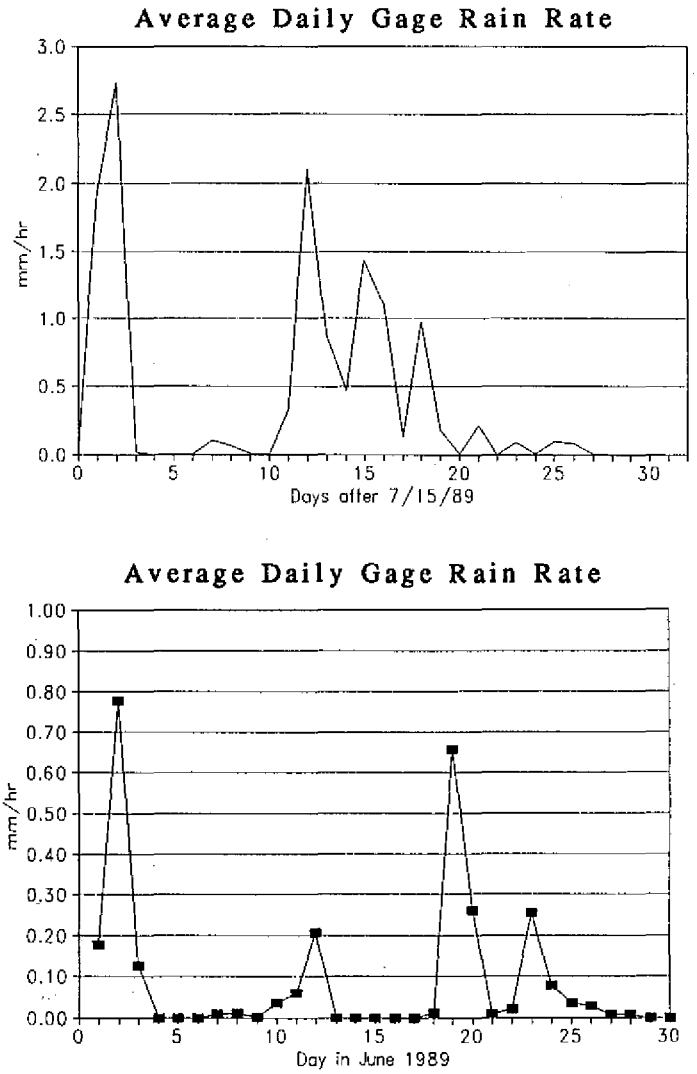

Fig. 5. Hourly accumulation of average gauge rain rates for all seven gauges for the June (a) and July-August (b) periods.

3.5 Z-R Relation

To convert the Z values to rain rate, R, a reflectivity-rain rate (Z-R) relation is needed. The form $Z=aR^b$, where Z is in mm^6/m^3 and R in mm/hr, is often used. The values of a and b depend on the drop size distribution, and hence are quite varied. This relation can be established empirically by fitting linearly coincident and contemporary reflectivity (dBZ) and rain gauge rain rate (R) data. Since the radar bin size and rain gauge resolution are site and radar-dependent, the Z-R relations are also site or radar dependent. Another approach examines the probability distribution of the reflectivity and gauge rain rate (Zawadzki, 1975, Rosenfeld *et al.*, 1991) and forces a non-linear fit to the pdf's of rain rate and reflectivity. These non-linear relationships, often presented in forms of look-up tables, are also range-dependent since the pixel sizes vary with range (Rosenfeld *et al.*, 1991).

Austin (1987) examined errors in establishing a Z-R relation and recommended that Z-R relations can be broadly classified into those for the convective, stratiform, and mixed rain type. The value of "a" ranges from 100 to 400 whereas "b" ranges from 1.25 to 1.6, both of which are dependent on the weather conditions. Wang *et al.* (1988) used the values a=200 and b=1.6 respectively which are derived from the Marshall-Palmer (1948) drop size distribution. During GATE, which had weather conditions similar to the Taiwan summer, the calibrated values of "a" and "b" are 230 and 1.25 respectively (Patterson *et al.* 1979). These sets of Z-R relations, termed respectively the Marshall-Palmer (MP) and GATE Z-R relations, are used to test the sensitivity of our calculations.

3.6 Monthly Radar Rain Rates

Using these Z-R relations, the cumulative histogram of rain rate at 4 km resolution was calculated. The radar noise levels were set at 18.5 dBZ to 19.5 dBZ (corresponding to about 0.5 mm/hr) for these reflectivity data and hence radar return values less than 19.5 dBZ were truncated.

The spatial distributions of the mean rain rate conditional on rain, based on the MP Z-R relation, for the June and July-August periods are shown in Figures 6a and 6b, respectively. In June, rain events are concentrated in the northern portion of the radar area and no rain events are detected for the southern portion of the radar area. In July-August, the average rain rates are fairly evenly distributed spatially. The spatial patterns also see a discontinuity across a sector in the NE direction. This reduction in radar reflectivity is due to the presence of the newly-built Hualien Concert and Conference Hall, which obstructs the radar beam.

The mean rain rates conditional on rain are 2.38 and 2.43 mm/hr, for the two periods, respectively. These values can be compared with the climatological mean rain intensities of about 2 and 3 mm/hr for June and July/August in Hualien (CWB, 1990). The areal mean rain rates, computed as products of the fractional rainy areas (see Section 3.3) and the rain rates conditional on rain, are 0.07 (0.10) mm/hr for the June period and 0.13 (0.18) mm/hr for July-August period based on the MP (GATE) Z-R relation.

3.7 Comparison with Other Satellite and Gauge Estimates

Wilheit *et al.* (1991) proposed a technique for estimating monthly rainfall over 5° latitude by 5° longitude areas from histograms of microwave brightness temperature computed from the Special Sensor Microwave Imager (SSM/I) on board the Defense Meteorological Satellite Program (DMSP) satellites. Their estimation technique is based on the assumption of lognormality of rain rate, the use of a combination of microwave channels to minimize the effect of water vapor, and a radiative model of the rain column. The DMSP SSM/I satellite

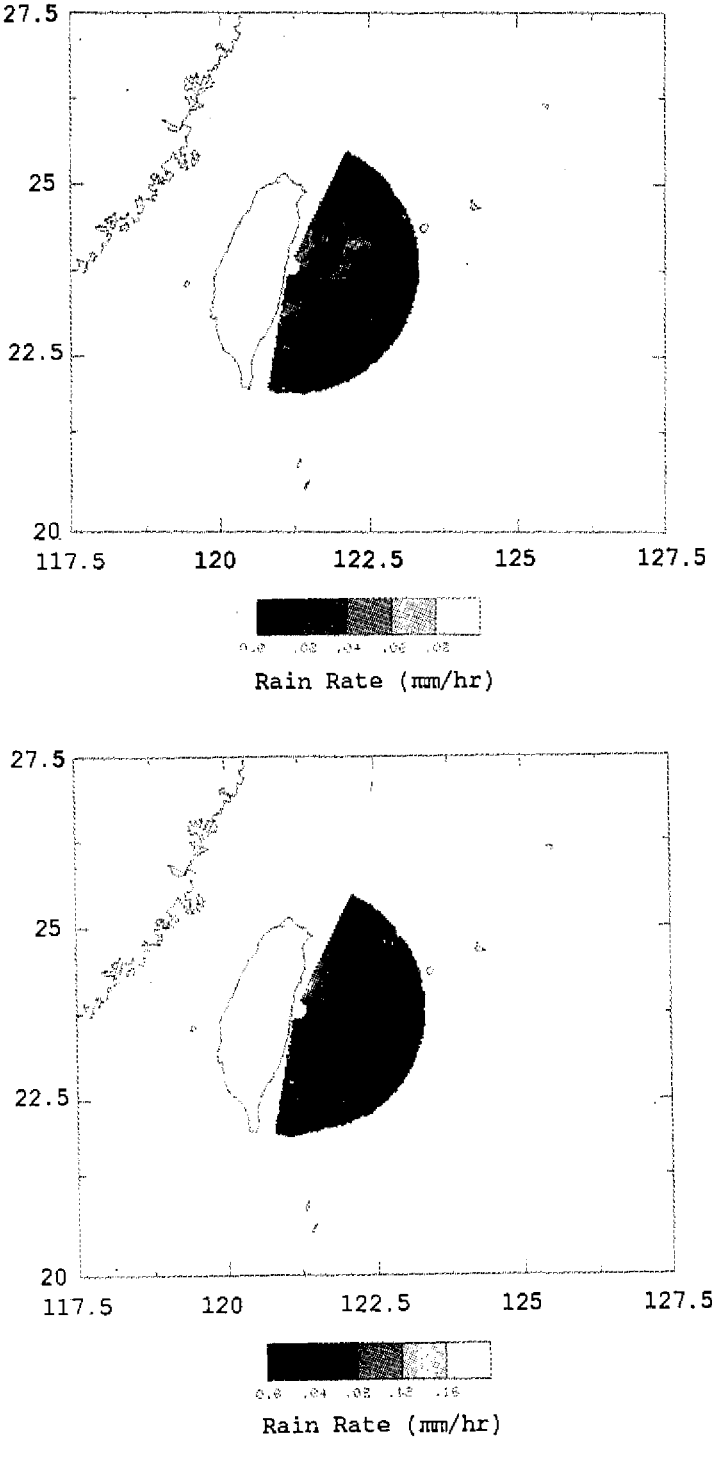

Fig. 6. Spatial distribution of the monthly mean radar derived rain rate for June 1989 (a), and July 15 - August 15, 1989 (b) periods. The Z-R relation $Z=200\ R^{1.6}$ is used.

is in a sun-synchronous orbit; observations are restricted to two narrow intervals of local solar time. For the Taiwan area, satellite passes occur at about 7 A.M. and 7 P.M. Monthly rainfall rates have been estimated using the A.M. passes, P.M. passes, and the combined daily data. The rain rates have been multiplied by a factor of about 1.8 to account for the "beam-filling" bias (Chiu *et al.*, 1990). The beam-filling error arises due to the non-uniformity of rain rates within the SSM/I sensor field of view and the non-linear rain rate-microwave brightness temperature relation.

Table 3 compares the radar-computed areal average means over the radar covered area and the means over the 5° by 5° box (20°-25°N, 120°-125°E) estimated from the Wilheit *et al.* technique, the GPI, and the gauge average rain rate. Despite the VIP levels used in the radar processing and the uncertainty in the Z-R relation, the monthly means compare favorably. The low radar rainfall rates in June compared to the July-August period is also reflected in the SSM/I and GPI estimates. The close match in the magnitude of the monthly rain rates is probably fortuitous, since the area covered is not exactly the same. The SSM/I estimates are restricted to the ocean area while the GPI include land area as well. A comparison of the SSM/I and GPI estimates is outside the scope of this study, and has been presented by Chiu *et al.* (1993).

Table 3. Comparison of Monthly Mean Rain Rate over the Taiwan Area. Units are in mm/month.

Technique	June	July	August
Radar mean			
MP Z-R	50	94	
GATE Z-R	72	130	
Rain Gauge Total	66	293	
SSM/I (20-25°N, 120-125°E)			
A.M	60	180	90
P.M	99	185	198
Mean	80	182	144
GPI(20-25°N,120-125°E)	70	194	226

4. RAIN AREA-AREAL RAINFALL RELATION

There exists a strong relation between the rain covered area and areal rainfall. Chiu (1988a,b) found that the area with rain rate above certain threshold, t, when appropriately chosen, explains over 98% of the variance of areal rain rate in the GATE area. Analyses of

precipitation over Texas, U.S.A., and Darwin, Australia lend further support to this statistical relation of tropical rain fields (Rosenfeld, *et al.* 1990). The optimal thresholds which maximize the variance explained for GATE are in the range of 4-5 mm/hr. A similar threshold of 5-7 mm/hr was obtained for Texas and Darwin (Rosenfeld, *et al.* 1990). Kedem *et al.* (1990b) and Kedem and Pavlopoulos (1991) showed that the slope of the regression is rather insensitive to the exact shape of the probability distribution of rain rate, and the threshold that maximizes the correlation is closed to the medium of the distribution. Kedem *et al.* (1990a) also pointed out that this linear relation between areas above a threshold and areal average rain rate can be quite general and is applicable to any meteorological fields which is related to rainfall. Hence once the climatological rain rate pdfs are known, the areal average rain rate can be faily accurately estimated from rain area.

The applicability of the linear relation, to some extent, depends on the relative constancy of the probability distribution of positive rain rates (Chiu, 1988, Kedem *et al.*, 1990, Atlas *et al.*, 1990). In Section 3.6, it was shown that the mean rain rates conditional on rain are relatively constant for the two periods: respectively 2.38 and 2.43 mm/hr. The production of DVIP levels by the radar processor also limits its applicability in detail quantitative rainfall estimation, but may be suited for the threshold method.

Linear regression analyses were performed on the hourly Hualien radar data with respect to rain areas above different rain rate thresholds. The results are shown in Tables 4 and 5. For the June period, the correlation coefficients peak at a threshold of t=2 mm/hr (R2=0.93) for the MP Z-R relation and 5 mm/hr (R2=0.89) for the GATE Z-R relation. For the July-August period, the correlations peaked at t=3 mm/hr (R2=0.93) for the MP Z-R relation and 10 mm/hr (R2=0.91) for the GATE Z-R relation. The slopes are also quite similar to those obtained from Texas and S. Africa (Rosenfeld *et al.*, 1990).

Table 4. Regression coefficients of area average rain rate on fractional area with rain rate greater than t. The MP Z-R relation $z=200\ R^{1.6}$ is used.

t	Intercept	Slope	R2	t	Intercept	Slope	R2
June 1 to June 30, 1989				July 15 to August 15, 1989			
1	0.003	3.02	0.84	1	-0.01	3.63	0.90
2	0.087	7.12	0.93	2	0.01	6.92	0.92
3	0.012	10.12	0.93	3	0.02	9.49	0.93
5	0.020	22.95	0.78	5	0.03	22.08	0.86
10	0.035	37.08	0.59	10	0.05	41.81	0.78
15	0.045	75.16	0.46	15	0.09	77.29	0.49
20	0.049	83.10	0.43	20	0.09	96.66	0.47

The time series of the areal average rainfall (A), spatial means (B) and standard deviations (s.d.s) (C) conditional on rain for the June and July to August period are shown in Figure 7. It is interesting to note that all these time series vary in phase: the higher the conditional rain rate, the higher the conditional rain rate variance.

Arkin's (1979) IR threshold technique has been applied to the area of overlap between the Hualien radar and GMS IR coverage. An IR rainfall index, defined similarly to the GPI

Table 5. Same as Talbe 4. except the GATE Z-R relation $Z=230\ R^{1.25}$ is used.

t	Intercept	Slope	R2
June 1 to June 30, 1989			
1	0.008	4.39	0.68
2	0.010	9.94	0.83
3	0.013	12.28	0.84
5	0.014	20.83	0.89
10	0.020	42.26	0.86
15	0.030	54.01	0.81
20	0.042	69.45	0.74

t	Intercept	Slope	R2
July 15 to August 15, 1989			
1	-0.01	5.63	0.80
2	0.02	10.11	0.85
3	0.01	12.14	0.88
5	0.04	19.48	0.88
10	0.03	39.15	0.91
15	0.05	53.45	0.89
20	0.06	76.81	0.85
25	0.10	126.29	0.61

as the product of the fraction area with IR temperature below the threshold of 235K (marked D in Figure 7) multiplied by the assumed climatological average rain rate of 3 mm/hr, is calculated. The low IR areas are delineated from the GMS imagery obtained from the GPCP AIP-1. Figure 8 shows the scattered plots of radar-derived rain rate versus the GPI rain rates for the June and July-August periods. The GPI rainfall index tends to over-estimate the radar rain rate. This over-estimate may be due to the use of a high mean rain rate conditional on rain. The mean rain rate of 3 mm/hr used in the GPI is estimated from the GATE data, which have a radar mean rain rate of about 4 mm/hr (Arkin, 1979). This is larger than the mean radar rain rates of about 2.4 mm/hr for the Hualien data.

5. SUMMARY AND RECOMMENDATIONS

An analysis of the radar statistics as a function of range showed a degradation of less than 1 dBZ at a range of 250 km. This result, in contrast to that obtained by Petty and Katsaros (1991) in the analysis of the TAMEX data, showed that range correction has been adequately applied. To reduce data storage, the radar processor only retains the maximum reflectivity of a column vector within the hour. The DVIP reflectivity data also limit many of its research uses. Since there are considerable vertical structures of reflectivity and variability within the hour in rain clouds, complete 15 minute volume scans should be stored for quantitative analysis. Finer dBZ scales should also be implemented.

Mean rain rates computed from reflectivity histograms show that they are sensitive to the exact Z-R relations used. The monthly mean rain rates are larger by about 50% when the GATE Z-R relation is used instead of the MP Z-R relation. The match between the rain rate and radar histograms are compromised by the differences in the spatial and temporal resolution of the radar and gauge data, and to the coarse digitization using DVIP levels. In addition, none of the rain gauges for our study are within the radar-covered area. The Z-R relation is fundamental to quantitative rainfall estimate; efforts to improve the Z-R relation should be emphasized. These will involve the finer digitization of radar reflectivity, implementation of a network of automated rain gauges, such as optical rain gauges, in remote ocean areas, recording at a frequency of at least every 15 minute. The rain gauge data should also be centralized for further processing.

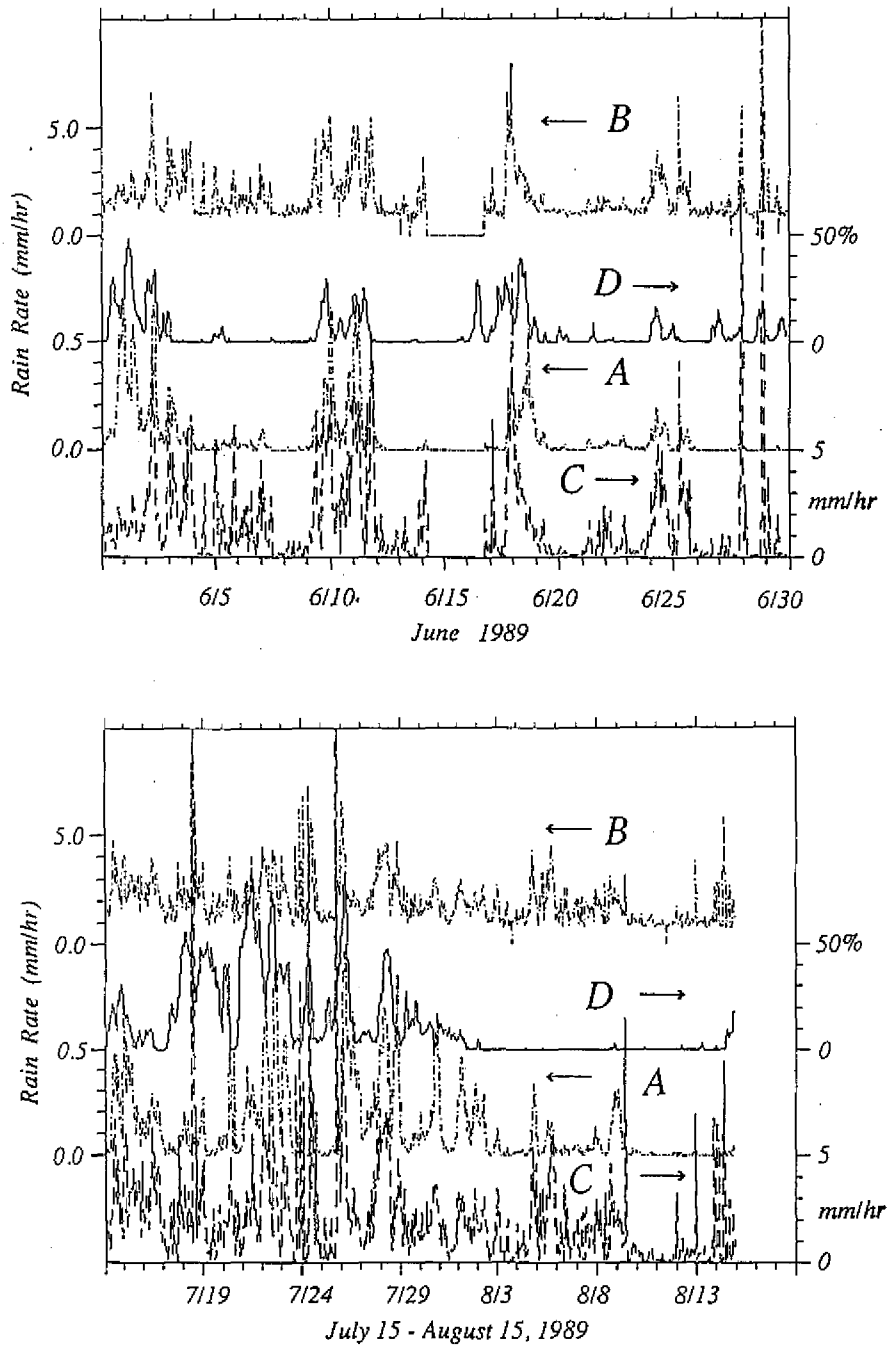

Fig. 7. Times series of the areal average rain rate (A), mean (B) and s.d. (C) of rain rate conditional on rain, and fraction of the area of the IR imagery in the radar covered sector north of 20°N with IR temperature less than 235°K (D) for June (Fig. 7a) and July-August (Fig. 7b) period.

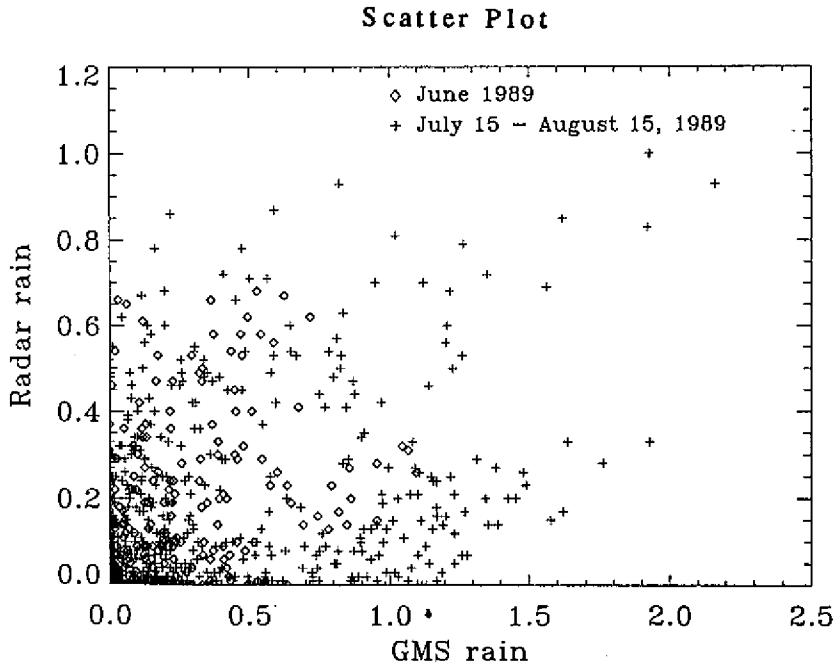

Fig. 8. Scattergram of GPI rain rate and radar derived rain rate for the area of overlap between IR imagery and radar coverage.

Maximum reflectivity values in excess of 55 dBZ occur in regions to the east and south east of Taiwan. Lacking a knowledge of the vertical distribution of reflectivity, extremely high rain rates are suspected. Comparison with IR imagery for the same period showed the absence of clouds over the high reflectivity areas, and hence the possibility of AP is suggested. The Central Weather Bureau has set up a station for the reception of digital IR and visible imagery data from National Oceanic and Atmospheric Administration (NOAA)'s Advance Very High Resolution Radiometer (AVHRR) and from Japan's Geostationary Meteorological Satellite (GMS). These data will prove to be extremely useful in rainfall analysis in Taiwan, as demonstrated here in the detection of AP.

Despite the use of DVIP reflectivity, the computed monthly radar rain rates over the radar-covered area using the MP and GATE Z-R relations, agree closely with other satellite and gauge estimates. The GPI, SSM/I, and radar estimates all showed a dry period in June, and a return to normal and wet condition later on in July and August, 1989.

The threshold technique for estimating areal rainfall has been tested using the available data. The results are encouraging in view of type of data available: maximum columnar DVIP reflectivity, recording for only the first 10 minute of the hour, and hourly gauge rain rate. The maximum variance explained is about 93% (90%), with optimal thresholds of about 2-3 (5-10) mm/hr for the MP (GATE) Z-R relation. The percentage of variance explained is less than those obtained from the GATE, Texas, and S. Africa data. The mean rain rates are, however, also smaller. These results are consistent with the theoretical results of Kedem *et al.* (1990b) who showed that the threhold technique works less well for low rain rates. If

the climatological rain rate distrubution is known, fairly accurate estimates of monthly areal averages in the Taiwan area can be anticipated.

Accurate rainfall estimates can have a profound impact on hydrological forecasting, flash flood warning, and typhoon monitoring in the Taiwan area. With the upgrade of the radar processing system, the implementation of automated rain gauge networks, the use of satellite imagery, and a commitment for the advancement of rainfall research, the potential contributions to environmental monitoring and weather forecasting in the Taiwan area can be enormous. These efforts will also contribute significantly to the international TRMM program.

Acknowledgments Thanks are due to the Central Weather Bureau of the ROC for providing the digital radar data and hourly rain gauge data and to the Global Precipitation Climatology Project Office for providing the GMS data for this study. Programming and graphic support provided by Hugh Powell, Janet Chien, and Vivien Kuan of General Sciences Corporation are gratefully appreciated.

REFERENCES

Arkin, P., 1979: The relationship between fractional coverage of high cloud and rainfall accumulation during GATE over the B scale, *Mon. Weath. Rev.*, **107**, 1382-1387.

Arkin, P., and B. Meisner, 1987: The relationship between large-scale convective rainfall and cold cloud over the western hemisphere during 1982-84, *Mon. Weath. Rev.*, **115**, 51-74.

Austin, P., 1987: Relation between Measured Radar Reflectivity and Surface Rainfall, *Monthly Weather Rev.*, **115**, 1053-1070.

Atlas, D., D. Rosenfeld, and D. Short, 1990: The estimation of convective rainfall by areal integrals. Part I: the theoretical and empirical basis. *J. Geophys. Res.*, **95**, 2153-2160.

Central Weather Bureau, 1990: Climatic Atlas of Taiwan, ROC, Vol I, C. Y. Tsay (Editor), CWB, Department of Communication, ROC.

Chiu, L.S. 1988a: Rain estimation from satellites: areal rainfall- rain area relation. Third Conference on Satellite Meteorology and Oceanography, Feb. 1-5, 1988, Anaheim, CA. 363-368.

Chiu, L. S., 1988b: Estimating areal rainfall from rain area, in Tropical Rainfall Measuring Mission. J. Theon, and N. Fugono, (editors), A. Deepak Publishing, 361-367.

Chiu, L. S. and B. Kedem, 1990: Estimating the exceedance probability of rain rates by logistic regression, *J. geophysical Res.*, **95**, D3, 2217-2227.

Chiu, L. S., G. North, D. Short, and A. McConnell, 1990: Rain estimation from satellites: effect of finite field of view, *J. Geophys. Res.*, **95**, 2177-2185.

Chiu, L. S., A. T. C. Chang, and J. Janowiak, 1993: Comparison of monthly rain rate derived from GPI and SSM/I using probability distribution functions, *J. Appl. Meteor.*, (to appear).

Doneaud, A.A, S. Ionescu-Niscov, D.L. Priegnitz and P.L. Smith, 1984: The area-time-integral as an indicator for convective rain volume. *J. Climate Appl. Meteor.*, **23**, 555-561.

Kedem, B., and L. Chiu, 1987: On the lognormality of rain rates, *Proc. Nat'l Acad. Sci.*, USA, **84**, 901-905.

Kedem, B., L. Chiu, and G. North, 1990a: Estimation of mean rain rate: application to satellite observations, *J. Geophys. Res.*, **95**, D2, 1965-1972.

Kedem, B., L. Chiu, and Z. Karni, 1990b: An analysis of the threshold method for measuring area-average rainfall, *J. Appl. Meteor.*, **29**, 3-20.

Kedem, B., and H. Pavlopoulos, 1991: On the threshold method for rainfall estimation: Choosing the optimal threshold level, *J. Amer. Stat. Assoc.*, **86**, 626-633.

Marshall, J. S., and W. M. Palmer, 1948: The distribution of raindrops with size. *J. Meteor.*, **5**, 165-166.

Moore, P. L., and D. L. Smith, 1979: Manually digitized radar data: interpretation and application, NOAA Technical Memorandum NWS SR-99, NOAA/NWS, Department of Commerce, Washington, D.C.

Patterson, V. L., M. D. Hudlow, P. J. Pytlowany, F. P. Richardson,, and J. D. Huff, 1979: GATE radar rainfall Processing system, *NOAA Tech. Memo.*, EDIS, **26**.

Petty, G., and K. B. Katsaros, 1991: Nimbus 7 SMMR Precipitation observations calibrated against surface radar during TAMEX. (To appear in J. Appl. Meteor.)

Rosenfeld, D., D. Atlas and D. Short, 1990: The estimation of convective rainfall by area integrals Part II: the height area rainfall threshold (HART) method. *J. Geophys. Res.*, **95**, D3, 2161-2176.

Rosenfeld, D., D. Wolff, and D. Atlas, 1991: General probability matched relations between radar reflectivity and rain rate, (Submitted to J. Appl. Meteor.).

Simpson, J., R. Adler, and G. North, 1988: A proposed Tropical Rainfall Measuring Mission (TRMM) satellite, *Bull. Amer. Meteor. Soc.*, **69**, 278-295.

Smith, P.L., L.R. Johnson, T.H. Vonder Haar and D. Reinke, 1990: Radar and satellite area-time-integral techniques for estimating convective precipitation. AMS Meeting, Anaheim, CA.

Wang, T.C.C., L.N. Chang and P.L. Lin, 1988: Rainfall estimates from digital radars in Taiwan area, in Tropical Rainfall Measurements, Ed. by J. S. Theon and N. Fugono, A. Deepak Publishing, 471-480.

Wilheit, T., A. Chang, and L. Chiu, 1991: Retrieval of monthly rainfall indices from microwave radiometric measurements using probability distribution functions, *J. Atmo. Oceanic Tech.*, **8**, 118-136.

Zawadzki, I., 1975: On radar-rain gage comparison, *J. Appl. Meteor.*, **14**, 1430-1436.